Geometry Characterization of Electroadhesion Samples for Spacecraft Docking Application

Mikela Ritter
USC Viterbi School of Engineering
3650 McClintock Ave.
Los Angeles, CA 90089
310-683-8530
mdritter@usc.edu

David Barnhart
Information Sciences Institute
4676 Admiralty Way, Suite 515
Marina del Rey, CA 90292
310-448-8644
barnhart@serc.usc.edu

Abstract—**Applications of electroadhesion include automation and inspection robots, consumer gripper devices, anchoring tools used in the military and biomedical industry, and more recently, mechanisms for spacecraft docking. The purpose of this study is to characterize geometries of electroadhesion samples for application in spacecraft docking and propose a metric to predict the interaction between geometry and captured object. Shear forces of electroadhesion samples composed of Kapton®Polyimide insulating material with embedded aluminum foil electrodes and three common space-rated substrate materials were measured. Responses of the electroadhesion samples configured in three geometries were identified using substrates attached to dynamic two-dimensional air bearing platforms. Geometries included a flat plate design as a prototype for cubesats, a concave, cylindrical design for potential application to circular, cylindrical spacecraft capture and torque mitigation, and a soft four-arm claw design as a prototype for docking to variable shaped objects with full coverage of object surface area. Quantitative and qualitative results were analyzed to characterize the optimal geometry for spacecraft docking. Surface area of each geometry, defined as the area of contact between electroadhesion samples implemented on the geometry and the substrate rigidly attached on air bearing platform, was compared to the stop time, defined as the time required for the geometry to mitigate both initial and residual motion of the air bearing platform. In summary, aluminized mylar substrate is identified as a superior type to achieve the highest attainable shear adhesion forces, and one electroadhesion geometry may be superior to others depending on specific docking scenarios in a space environment in agreement with the proposed metric.**

Table of Contents

1. Introduction

The use of electroadhesion in engineering has developed in industrial applications including automation and inspection robots, biomedical markets including lab automation and bandages, military devices including pads for wall-climbing soldiers and smart vehicle door seals, consumer gripper devices, and now potentially in space applications including micro-inspection robots, anchoring tools for human EVA, and spacecraft docking mechanisms [1]. In recent years, electroadhesion have been evaluated in space applications, specifically as docking mechanisms, by NASA Marshall Space Flight Center, the SPHERES system by MIT Space Systems Laboratory [2], the Stanford Research Institute (SRI), and the Defense Advanced Research Projects Agency (DARPA). In addition, electroadhesives are now being offered commercially by companies including Grabit, Inc [3].

This section of the paper summarizes previous research in and the current state of electroadhesion technology. Section 2 outlines the experimental setup and procedure. The results and discussion are presented in Section 3, including a computer-aided design (CAD) model of the air bearing platforms used for dynamic testing with docking geometries, and figures of static and dynamic measurements. Section 4 summarizes the paper.

Spacecraft docking mechanisms began as essential developments in capturing disabled spacecraft and safely docking crew vehicles during the lunar landing missions by NASA and Russia. Various capture techniques for disabled spacecraft have included a variety of mechanisms including spears thrusting into a cavity, nets cast around an object, adhesive strips to attach to an object, and probes into rocket nozzles such as in the Space Shuttle missions, and the Remote Manipulator System such as on the International Space Station [1].

Electroadhesion as a spacecraft docking mechanism requiring minimal power uses an electrostatic force produced with adjacent planar electrodes, each induced with positive or negative charge. An electric field across the electrodes, consisting of large voltage (kilovolts) and small current (nanoamps), induces opposite charges on a substrate generating an electrostatic adhesion phenomenon as shown in Figure 1.

An electroadhesion sample is composed of an electrode configuration embedded within an insulator material. Common insulating materials include polymers such as silicone, polyurethane, and polypropylene sheets with maximum shear force efficiencies specific to each material and varying with different attached substrates [4]. For the purpose of this experiment, aluminum electrodes and Kapton®polyimide as a space-rated insulating material will be considered. Each electrode in the electroadhesion sample is induced with a positive or negative charge using high voltage, as shown in Figure 1. Resulting in an induced electric field, the substrate placed adjacent to the active electroadhesion sample is characterized by opposing charges, and an electroadhesion phenomenon is produced [4]. The attachment substrate may be a conductive or insulating material. For a conductive substrate, electrons on the surface are free to move and an electric field is induced

978-1-5090-1613-6/17/31.00 ©2017 IEEE

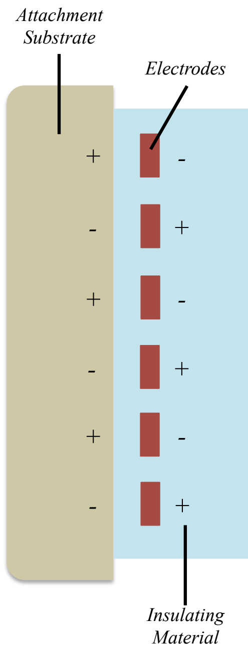

Figure 1. **Schematic of attached substrate and sample activated by high voltage applied to electrodes inducing electroadhesion effects.**

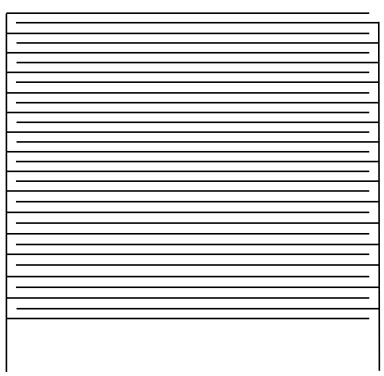

Figure 2. **Electroadhesion sample electrode configuration.**

by Lorentz forces producing the attraction between substrate and clamping material. For nonconductive substrates, an electrostatic attraction force between substrate and clamping material is induced by electrical and molecular polarization effects in the substrate material [4].

The electrode configuration in Figure 2 is characterized by superior shear adhesion forces in comparison to other electrode configurations [4].

The normal pressure, P_N, produced between the electroadhesion sample and substrate by an applied voltage e is derived as

$$P_N = \frac{\epsilon_0 \epsilon_c e^2}{2\left(2d\right)^2} \tag{1}$$

where ϵ_0 is the dielectric constant of a vacuum, ϵ_c is the relative dielectric constant of the clamping material, d is the thickness of the electrode, and l is the lateral distance of separation between the positively and negatively charged electrodes embedded within the clamping material. The shear pressure, P_S, is given in terms of the normal pressure as

$$P_S = \mu_s P_N \tag{2}$$

where μ_s is the coefficient of static friction between the electroadhesion sample insulating material and substrate. Normal and lateral pressures are maximized with electrodes of minimal thickness and a minimal lateral distance between the oppositely charged electrodes. Electrodes should be configured a minimum distance $l_{min} = e_{max}/\epsilon_s$ apart, for dielectric strength of clamping material ϵ_s, to prevent short circuiting and neutralization of the clamping material.

2. EXPERIMENT

This study primarily quantified the shear forces of planar electroadhesion samples composed of space-rated insulating material Kapton®polyimide attached to three common space-rated materials as substrates including bare aluminum, anodized aluminum, and aluminized mylar. Further, application of the study included quantitative and qualitative analysis of soft and hard structured electroadhesion geometries. Experimental geometries were docked to aluminum substrates rigidly attached to a two-dimensional air bearing platform with 3-degrees of freedom as a sample spacecraft docking response mechanism.

Static Response

Kapton®polyimide adhesive-back film by DuPont USA was used to insulate Reynolds Wrap Heavy Duty Aluminum Foil electrodes cut with a precise exacto knife. The electrodes were manually cut into the configuration shown in Figure 2. A power supply connected to an XP Power DC to HV DC Converter by EMCO produced a maximum voltage of $5\ kV$ to be input to the electroadhesion samples. Insulating material thickness was dependent on product availability. Minimal available thickness of $0.001''$ was chosen to achieve the highest allowable shear forces [4]. Electroadhesion samples were activated by a power source and DC to HV DC amplifier, connecting one electrode to positive voltage, one electrode to negative voltage, and the insulating material to ground. Activated samples were then attached to one of three tested substrate materials including bare aluminum, anodized aluminum, and aluminized mylar. Using a spring balance, the maximum applied shear force before slippage occurred was measured over varying input voltages within range of $0 - 5\ kV$. Before each measurement was acquired at a stepped-up voltage, the electrodes were grounded and aluminum foil was placed between the substrate and electroadhesion sample to discharge static electricity. This testing process was repeated for each of the three substrate materials.

Dynamic Application

Three electro adhesion sample geometries were proposed [3], and two were experimentally tested with Kapton®Polyimide electroadhesion samples. Further testing may include geometries composed of Polypropylene electroadhesion samples, and variable geometries. The electroadhesion geometries designed to experiment with spacecraft docking applications are shown in Figure 4.

The characteristics of hard and soft structure configurations were measured and analyzed with rigidly attached, aluminum substrates on an air bearing platform. The experiment setup for the dynamic application of the electroadhesion samples is shown in Figure 5. Electroadhesion geometry (1) is shown

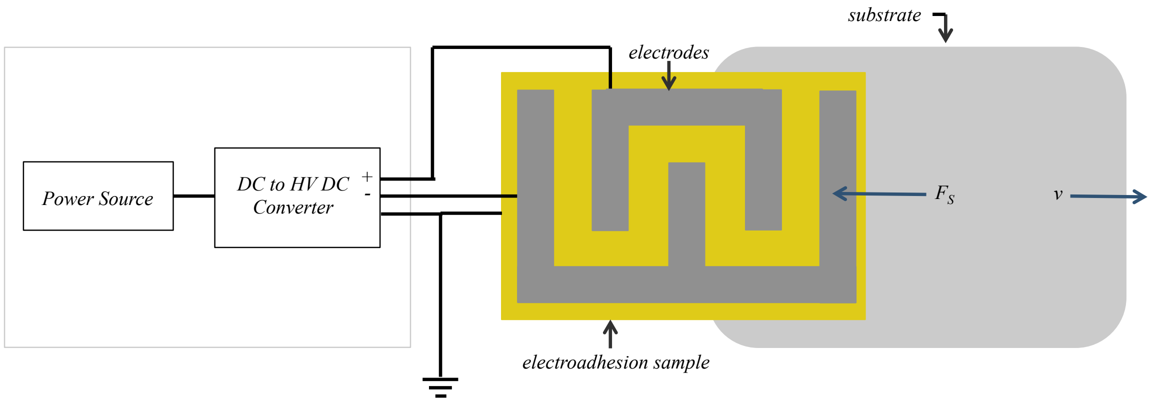

Figure 3. Experimental setup of electroadhesion sample with substrate to measure shear force F_S.

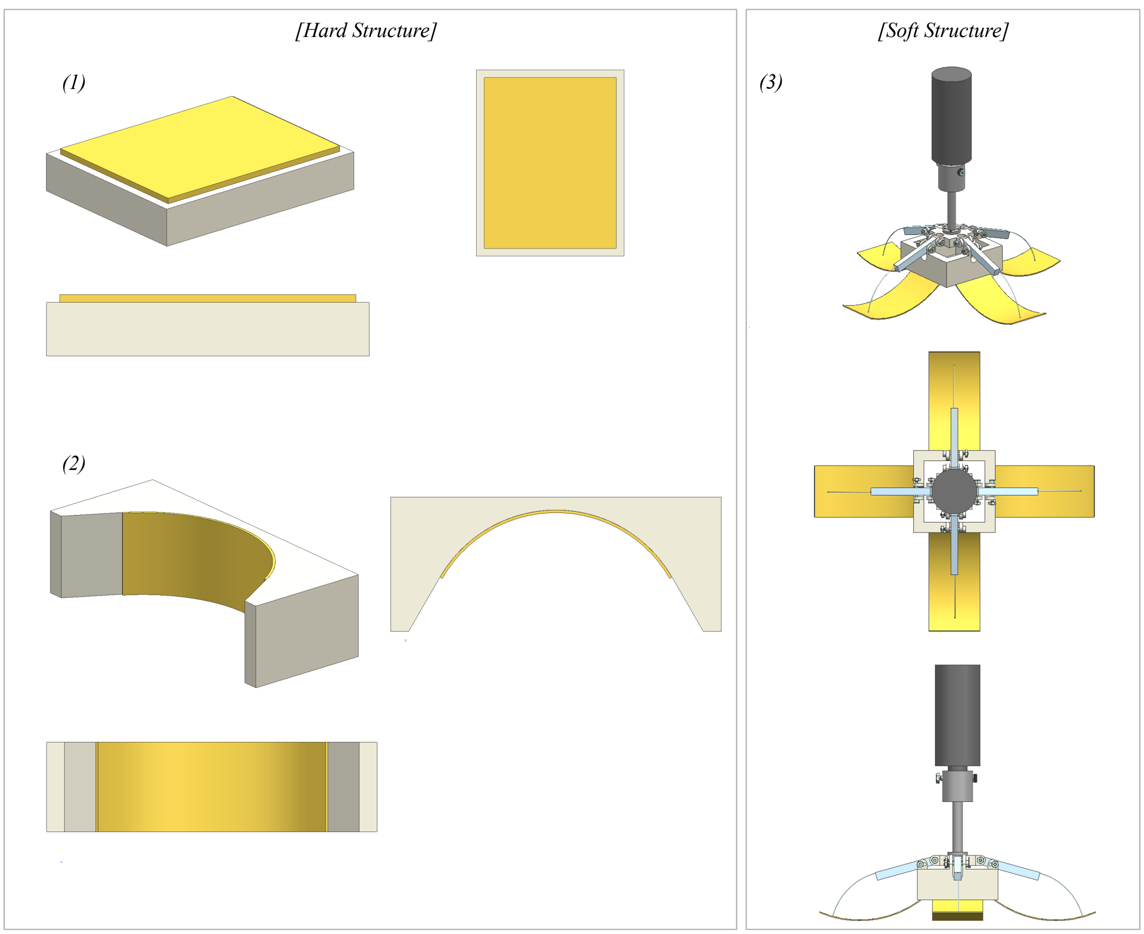

Figure 4. Hard structure (left) and soft structure (right) geometries of electro adhesion device in isometric, top, and front views.

as a flat plate in Figure 4, which was dynamically tested with a flat aluminum plate attached to the side of the air bearing platform, as shown in the experimental setup in Figure 5. Geometry (2) show as a cylindrical concave geometry of equal radius to the cylindrical air bearing platform was tested with an aluminum piece wrapped directly over the air bearing platform. Geometry (3) will be tested with an extended aluminum ball from the air bearing platform. Quantitative results for this geometry are variable and testing is a continuing process.

Initial distance of the air bearing platform to the electroadhesion geometry and the time that the platform traveled to reach an adjacent position was measured. For dynamic application testing, the air bearing platforms provided a small velocity on a vector that would interest the EA sample. The approach velocity, assumed constant, of the air bearing platform to the geometry was calculated as the distance over the time traveled. Measurements of time for the air bearing platform to stop initial motion from the approach velocity and residual motion from impact were acquired. Additionally, a qualitative analysis on the behavior of the air bearing platform with each activated electroadhesion geometry was executed with a rating of ability to stop the platform on a scale of 1 to 3, from poor, medium, and excellent.

3. Results and Discussion

Static Response

Consider Figure 6 showing the experimental results for measured shear forces between electroadhesion samples and three substrate materials at various input voltages. Experimental shear forces are expected to be less than the predicted values as a result of air pockets between the sample and substrate reducing the strength of attractive forces.

Additionally, samples were made by hand. With fabrication techniques of 3D printing, vapor deposition, or chemical etching, and the metal electrodes designed in an intricate circular configuration [5] onto the insulating material, shear forces are expected to be greater than those attained in this experiment. Further testing of geometries may include experiments in a vacuum chamber to obtain expected forces in a space environment with application to spacecraft docking. Electroadhesion samples produce strongest adhesion forces in a vacuum environment where sample and substrate can adjacently attach without pocketed air between.

Further, the general trend of the experimental results is similar to that of the predicted values. As expected, the flexible Aluminized Mylar substrate most efficiently conformed to the shape of the electroadhesion sample, with minimal air pockets, in comparison to the rigid plates of aluminum and anodized aluminum substrates. Large air pockets between the rigid substrate materials and electroadhesion samples prevented direct contact, reducing the measured shear pressure.

Dynamic Application

Three geometries of the electroadhesion samples shown in Figure 4 were constructed. One geometry consisted of a rectangular plate configuration to dock to the attached aluminum plate on the air bearing platform, representing the side of a cubesat or rectangular spacecraft. Another geometry consisted of a concave, cylindrical shape to dock directly to the cylindrical air-bearing platform, applicable to cylindrical, rotating spacecraft. The final geometry consisted of a soft structure with electroadhesion samples attached as four arms on a clamp [3], closing around a contact point of an aluminum spherical ball like a soft hand. The soft claw geometry allows for docking to a variety of shapes, potentially as smaller parts on a spacecraft. Table 1 compares results of the dynamically tested geometries with measured surface area defined as the contact area of electroadhesion sample implemented on the geometry and the substrate object. The time for the geometry to stop initial and residual motion, t_{f0}, of the air bearing platform with an initial velocity of $2\frac{cm}{s}$, and a qualitative analysis on the ability of the geometry to stop the motion of the platform is also presented in Table 1.

Table 1. Comparison of characteristics of three electroadhesion geometries including contacting surface area, time to stop motion of air bearing platform with electroadhesion forces, and qualitative ranking of the geometry's ability to stop motion of the platform. Results were acquired with approach velocity of $2\frac{cm}{s}$.

Geometry	(1) Plate	(2) Concave	(3) Claw
SA $[cm^3]$	122.5 ± 0.6	44.3 ± 0.6	280 ± 30
t_{f0} $[s]$	2.06 ± 0.05	28.81 ± 0.05	Variable
Ability	2	1	Variable

As expected, the time to mitigate the initial and residual motion of the air bearing platform with the geometries is proportional to the surface area: $t_{fo} = f(SA)$. The flat plate geometry, with greater surface area than the concave geometry, mitigated the motion in less time and more efficiently with less residual motion than the concave geometry. The ability of the soft claw geometry to stop the motion of the platform is to be determined, as the contact surface area is variable on the shape of the substrate object. Dynamic testing was conducted with an input voltage of 3 kV to the electroadhesion samples. Future testing to acquire a larger data set may quantify the surface area in relation to shear force $F = P_N \cdot SA$, inputing variable voltages to the samples in order to achieve variable shear pressure P_N. A qualitative study using lagged aluminized mylar on the air bearing platform was significantly more efficient than the hard-structured aluminum substrate.

Consider Figure 7 comparing the impact velocity v_f of the air bearing platform approaching the flat plate or concave geometries and the time until motion of the platform has stopped, t_{f0}. Notice at lower approach velocities, v_f, for the concave geometry the time to stop was shorter than at higher approach velocities, as expected since the change in momentum of the platform is proportional to its acceleration. It was qualitatively observed that at higher approach velocities, residual motion had larger effects than at lower approach velocities. A linear relationship between the approach velocity and stop time for the concave geometry was observed.

Stop times for the flat plate geometry varied from the concave geometry. The platform with a larger approach velocity of 2.4 ± 0.6 cm/s was characterized by a smaller stop time $t_{f0} = 2.06 \pm 0.05$ s in comparison to an approach velocity of 1.0 ± 0.3 cm/s with stop time $t_{f0} = 1.70 \pm 0.05$ s. This may be a result of additional residual motion of the air bearing platform caused by a small angle $\theta > 0$ between normal vectors of the plate and substrate. Further experimentation with samples characterized by stronger adhesion forces is necessary to determine the relationship between the approach

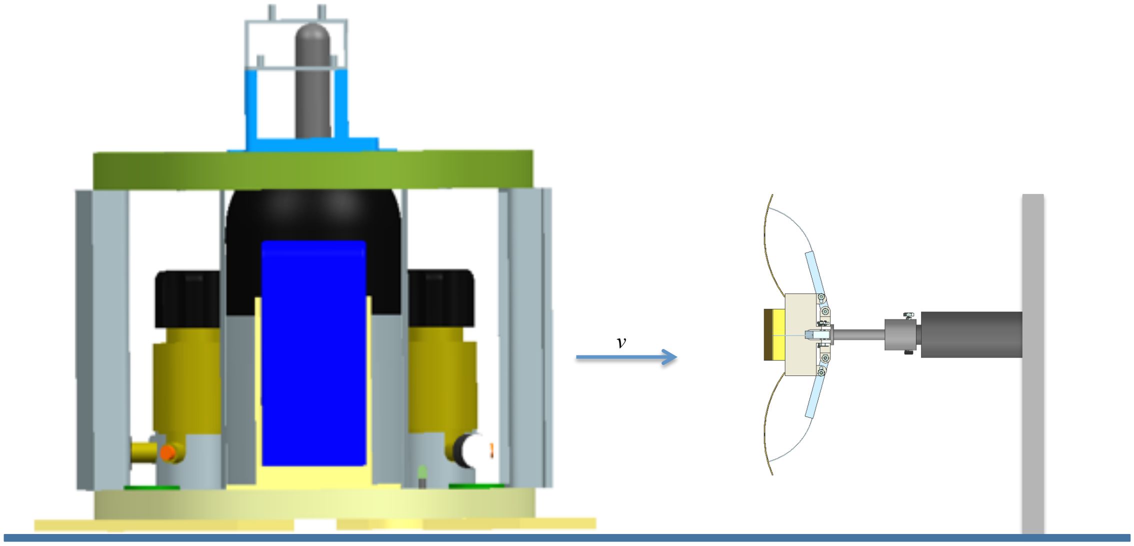

Figure 5. **Experimental setup of air bearing platform with attached substrate and electroadhesion device of geometry (3), Figure 4, connected to a power source with a DC to high voltage (HV) DC converter.**

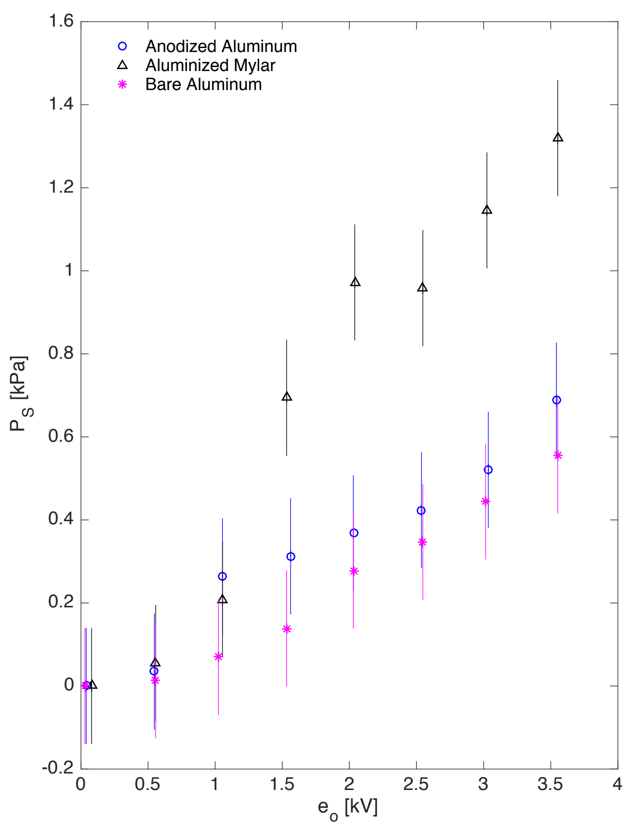

Figure 6. **Static shear pressure of electroadhesion samples with three substrates measured at various electrode voltages.**

velocity and stop time for the plate geometry.

In summary, it was observed that the stop time for a larger contact surface area (flat plate geometry in this case) was less than the stop time for a smaller contact surface area (concave geometry in this case). Due to limitations of the hand made electroadhesion samples which produced forces on the order of 1 N, a clear relationship between stop times for the plate geometry over an input range of velocities $1.2 \leq v_f \leq 2.5$ could not be determined. However, a linear relationship between stop time and approach velocity for the concave geometry was observed.

Proposed Metric for Capturing

Electroadhesion used for the capture of objects provides contact that translates to the space environment, through a combination of the contact geometry and the normal force to stop relative velocity and maintain contact. The most efficient use of electroadhesion activation to achieve the maximum contact between sample and captured object, is to provide at least two (and preferably more) parallel and opposing surfaces in the geometry that use shear. While there are an endless number of geometries that might be considered, a two-dimensional metric is proposed to begin to explore levels of ”goodness” for a particular electroadhesion geometry. This is defined as the ratio of the angle α between two opposing shear forces acting on the captured object to the area of contact between the sample geometry and the object. We define the normal shear force vector as positive in the direction perpendicular to the sample, pointing against the initial motion from the target to the capture point from the sample geometry. Figure 8 shows the notional layout and morphology. For example, a simple flat plate implemented with the electroadhesion sample has only one geometry that has been rigidly set in an initial position relative to a captured object. In this experiment, the second geometry is set at angle of $\alpha = 0$ rad from the first geometry because it does not exist and the plate is essentially π rad or flat to the object. There is essentially only one shear force acting on the captured object. Now consider an angle of $\alpha = \pi$ rad as the optimal angle, since both samples are exactly orthogonal to the captured

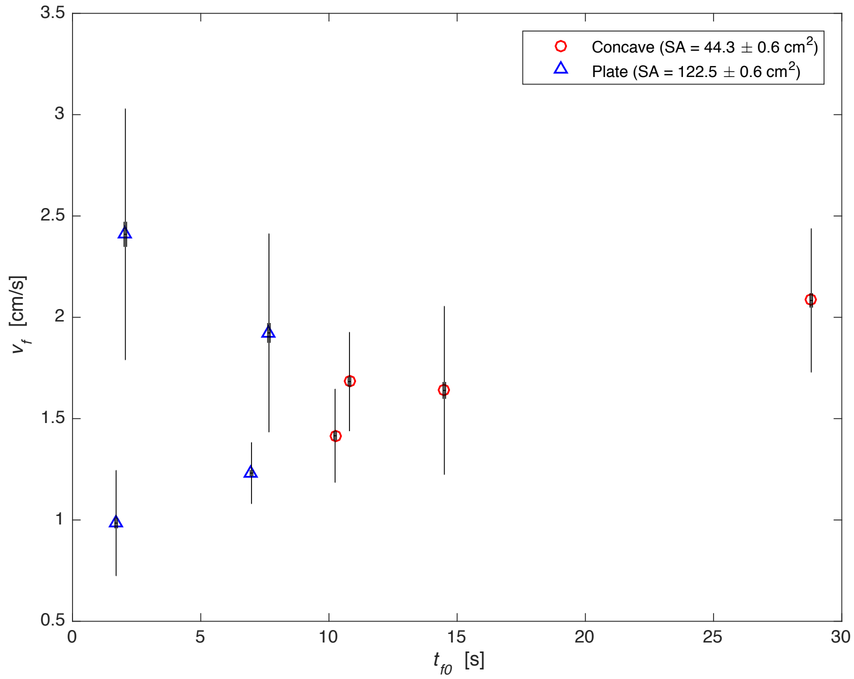

Figure 7. **Comparison of time for electroadhesion geometry to stop movement (initial and residual), t_{f0}, of the air bearing platform with approach velocity v_f.**

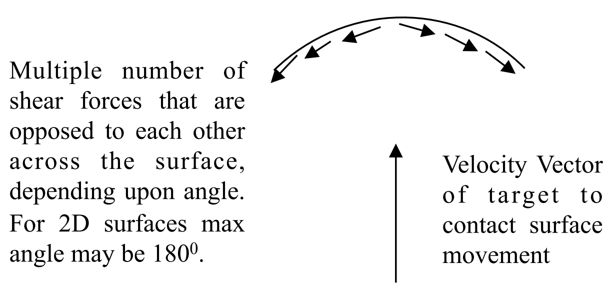

Figure 8. **Notional layout and morphology of proposed capturing metric.**

object and facing the object. A geometry at this angle is characterized by maximum opposing direction shear forces attained over the contact area of both samples and object.

While this begins to identify how to validate a capture dynamic using electroadhesion, it does not take into account the potential complexity of shapes between the electroadhesion contact surface and a target. Consequently, a two-dimensional metric is proposed to quantify and normalize the curvature of each sample geometric interaction, between contact surface and target. Define a geometry that encapsulates exactly half of the captured object as $\beta = 1$, such as a concave cylinder of π rad. Then, the geometry used in this experiment as a concave cylinder of $\frac{2}{3}\pi$ rad is defined as $\beta = \frac{2}{3}$. The flat plate geometry is defined as $\beta = 0$ because the plate has an infinite radius of curvature. Further, a third geometry, the clamp, has been proposed [3] with three-dimensional shear force capturing capabilities (see Figure 9). A three-dimensional metric is continually being explored and experimentally tested (see Figure 10). Additional testing will include varying the angle α by capturing the air-bearing platform between two geometries. In summary, each electroadhesion geometry in dynamic application will be characterized by angles α and β to predict the efficiency of capturing abilities.

4. CONCLUSIONS

One electroadhesion geometry may be superior to others depending on specific scenarios in a space environment. In an atmosphere of standard pressure and temperature, shear adhesion forces of the electroadhesion samples on three substrate materials were one magnitude smaller than theoretically predicted. General trends of experimental results for each substrate material agreed with those predicted by theory. The relationship of the time to stop the initial approach velocity and residual motion of an air bearing platform and the surface area of contact between the electroadhesion sample and substrate was determined for the concave geometry as linear. In application, specific geometries are superior depending on the spacecraft or object shape. Additionally, the contact surface area between the geometry samples and spacecraft is a determining factor in the ability of the geometry to stop the spacecraft motion. In summary, as a low mass, low power device, electroadhesion geometries may provide superior, useful alternatives to predetermined mechanical docking systems through optimization of sample fabrication and geometries in further studies.

5. FURTHER INVESTIGATION

Further investigation may include measuring the shear forces of electroadhesion samples composed of different insulating materials such as polypropylene and mylar with varying substrates. Testing additional sample geometries for specific spacecraft shapes using computer-printed samples may in-

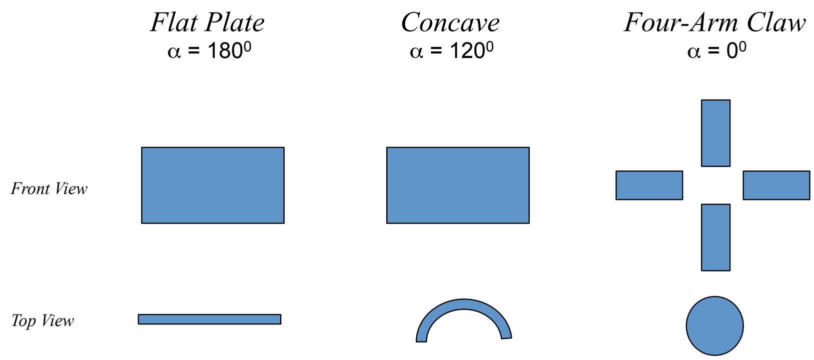

Figure 9. Defined angle α for geometries with application to spacecraft docking and object capture.

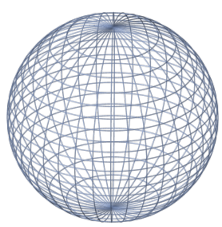

For a 3D surface, number of shear forces that could oppose each other is greater than 180^0, and the third dimension allows for increased contact resistance to movement.

Figure 10. Proposed three dimensional metric for electroadhesion geometries.

crease the efficiency and performance of the electroadhesion devices for spacecraft docking application. In addition, a system metric may be defined associating a balance force for shear with contact surface area in which the balance accounts for the opposing shear forces from the curvature of geometry surfaces. The shear normal force can be normalized to quantify a specific shear normal factor. Moreover, testing to validate a specific area versus geometry may help identify hybrids that support different structures or inform possible electroadhesion contact posts for future spacecraft. Future testing in a vacuum chamber may also mitigate effects from air pockets trapped between substrate and sample during shear force measurement acquisition. In this case, experimental measurements are expected to be closer to theoretical predictions than were determined in this study.

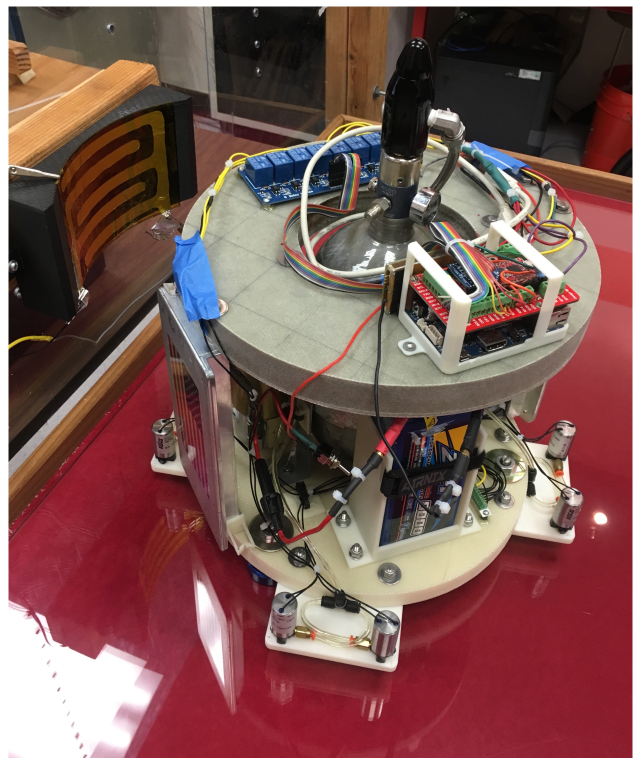

Figure 11. Isometric view of air bearing test platform with concave geometry and electroadhesion sample activated.

APPENDIX

Images of dynamic testing the concave geometry are shown in Figures 11 and 12 with the air bearing platform.

ACKNOWLEDGMENTS

This research was supported by the Space Engineering Research Center at the Information Sciences Institute under the Viterbi School of Engineering at the University of Southern California. The authors would like to thank the Stanford Research Institute, and especially Dr. Samson Phan, for their input on previous electroadhesion research and in efficiently crafting electroadhesion samples. Additionally, the authors are grateful for the help of William Valliant of the Viterbi School of Engineering and Michel Sika of the Information Sciences Institute on the electronics of the project. The authors appreciate the help of Dr. Donald Ruffatto and Dr. Aaron Parness of the Jet Propulsion Laboratory for their input on final details of the paper.

REFERENCES

[1] T. Bryan, *et al.*, ”Innovative Electrostatic Adhesion Technologies,” NASA Marshal Space Flight Center, Huntsville, AL, Stanford Res. Inst., Stanford, CA.

[2] Massachusetts Int. of Technology Space Systems Laboratory. (2014). *SPHERES.* Web. Available: http://sl.mit.edu.

[3] DesignCo Marketing. (2015). *Grabit, Inc.* Web. Available: http://www.grabitinc.com.

[4] J. P. Tellez, *et al.*, ”Characterization of Electro-adhesives for Robotic Applications,” in Int. Conf. Robotics and

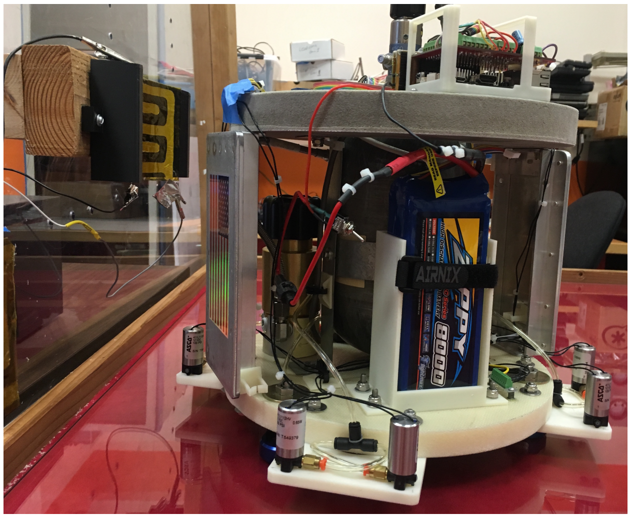

Figure 12. **Side view of air bearing test platform with concave geometry and electroadhesion sample activated.**

Biomimetrics, Karon Beach, Thailand, 2011.

[5] D. Ruffatto III, *et al.*, "Increasing the adhesion force of electrostatic adhesives using optimized electrode geometry and a novel manufacturing process," Journal of Electrostatics, 2014, pp. 146 - 155.

[6] R. Pelrine, "Electroadhesive Wall Climbing Robots and more," Microrobot Inspectors. Stanford Res. Inst., Stanford, CA, 2009.

[7] H. Allison *et al.*, "Electro Adhesion Device," U.S. Patent 6 791 817 B2, Sep. 14, 2004.

[8] D. F. Ruffatto III, "Hybrid Electrostatic and Micro-Structured Adhesives for Robotics Applications," Illinois Institute of Technology, Chicago, IL, 2015.

[9] D. Ruffatto III and M. Spenko, "Parameter Optimization of Directional Dry Adhesives for Robotics Climbing and Gripping Applications," in IEEE Int. Conf. Robotics and Automation, Saint Paul, MN, 2012.

[10] D. Ruffatto III, *et al.*, "Optimization and Experimental Validation of Electrostatic Adhesive Geometry," in IEEE Aerospace Conf., Big Sky, MT, 2013.

[11] D. Ruffatto III, *et al.*, "Experimental Evaluation of Adhesive Technologies for Robotics Grippers on Micro-Rough Surfaces," IEEE Int. Conf. Robotics and Automation, Hong Kong, China, 2014.

[12] M. Dadkhah, *et al.*, "A Self-Aligning Gripper Using an Electrostatic/Gecko-Like Adhesive," IEEE Int. Conf. Intelligent Robots and Systems, Daejeon, Korea, 2016.

BIOGRAPHY

Mikela Ritter *is a senior undergraduate earning a B.S. in Astronautical Engineering with a minor in Mathematics at the University of Southern California. She is currently a research student at the Space Engineering Research Center. Her current research activities include electroadhesion technology and flexible walls in confined flow. She is currently applying to doctoral programs for enrollment in the fall of 2017 to continue her research endeavors in advancing the scientific frontier.*

David Barnhart *is currently an active Research Professor in the Department of Astronautical Engineering at USC, and the Director/ Co-Founder of the USC Space Engineering Research Center. He is also CEO and co-founder of Arkisys Inc., a global space engineering and general contracting startup for small to large space platforms on orbit. David holds a Bachelor of Science degree in Aerospace Engineering from Boston University and a Masters of Engineering from Virginia Polytechnic Institute. At USC, he specializes in developing innovative technologies and architectures for 2nd generation space morphologies, satellite robotics and inspiration-based engineering techniques through hands-on projects with students, faculty and staff amongst the various Schools at USC, with outreach to industry based on the "engineering teaching hospital" construct.*